Proliferative cells in the rat developing neocortical grey matter: new insights into gliogenesis

Ramona Frida Moroni[a], Francesco Deleo[a], Maria Cristina Regondi[a], Laura Madaschi[b], Alida Amadeo[c] and Carolina Frassoni[a]

[a]Unit of Clinical and Experimental Epileptology, Fondazione I.R.C.C.S. Istituto Neurologico "C. Besta", Milan, Italy; [b]UNITECH NOLIMITS, University of Milan, Italy; [c]Department of Biosciences, University of Milan, Italy

Corresponding author:
Ramona Frida Moroni
Unit of Clinical and Experimental Epileptology,
Fondazione I.R.C.C.S. Istituto Neurologico "C. Besta",
Via Amadeo 42,
20133 Milano, Italy
Phone: +39-02-2394615
e-mail: ramona.moroni@istituto-besta.it

ABSTRACT

The postnatal brain development is characterized by a substantial gain in weight and size, ascribed to increasing neuronal size and branching, and **to** massive addition of glial cells. This occurs concomitantly to the shrinkage of VZ and SVZ, considered to be the main germinal zones, thus suggesting the existence of other germinative niches. The aim of this study is to characterize the cortical grey matter proliferating cells during postnatal development, providing their stereological quantification and identifying the nature of their cell lineage. We performed double immunolabeling for the proliferation marker Ki67 and three proteins which identify either astrocytes (S100β) or oligodendrocytes (Olig2 and NG2), in addition to a wider panel of markers apt to validate the former markers or to investigate other cell lineages. We found that proliferating cells increase **in number** during the first postnatal week **until P10** and **subsequently decreased until P21**. Cell lineage characterization revealed that grey matter proliferating cells are prevalently oligodendrocytes and astrocytes along with endothelial and microglial cells, while no neurons have been detected. Our data showed that astrogliogenesis occurs prevalently during the first 10 days of postnatal development whereas, contrary to the expected peak of oligodendrogenesis at the second postnatal week, we found a permanent pool of proliferating oligodendrocytes enduring **from birth until P21.** These data **support the relevance of glial proliferation within the grey matter** and could be a point of departure for further investigations of this complex process.

INTRODUCTION

The generation of cell types in the cortex occurs in temporally distinct, albeit overlapping, phases. It is widely reported that the neurons that populate the adult murine cerebral cortex are born prenatally (Bayer et al. 1993; Parnavelas 2000; Hevner 2006), whereas gliogenesis is mostly postnatal (Levison et al. 1993; Parnavelas 1999; Bandeira et al. 2009; Ge et al. 2012; Ge and Jia 2016). Cortical neurogenesis begins with the production of deeper projection neurons (embryonic day (E)**15–E17 in rat**) from radial glial cells (RGCs) residing in the ventricular zone (VZ) (Parnavelas 2000) and continues with successive generation of superficial projection neurons (**E17–E21**) from intermediate progenitor cells (IPCs) residing in the subventricular zone (SVZ) **(Bayer et al. 1993**; Noctor et al. 2004; Franco and Muller 2013). Cells originating from SVZ at late embryonic days and early postnatal life (in rat between E17 and postnatal day (P) 14) are destined predominately for glial lineage. Astrocytes are first detected around E16 and oligodendrocytes around birth; however, the vast majority of both cell types are produced during the first month of postnatal development (Sauvageot and Stiles 2002; Bayraktar et al. 2014; Tabata 2015), when the main germinal zones VZ and SVZ shrink dramatically. Considering that glial number in the cortex increases six to eightfold from birth to P21 (Bandeira et al. 2009), these findings suggest that there is a population of cycling cells outside VZ and SVZ, most likely in the CNS cortical parenchyma. **At** this regard, Ge and co-workers (2012) observed frequent symmetric cell division of protoplasmatic astrocytes during the first postnatal days, and obtained evidence supporting that a major source of glia in the mouse postnatal cortex is the local proliferation of differentiated astrocytes. Intriguingly, cell quantification revealed also a marked neurogenesis in the early postnatal cerebral cortex (Lyck et al. 2007; Bandeira et al. 2009), implying that the neurons found in the adult brain are not necessarily generated during embryonic development.

In light of the foregoing findings, new attention should be paid at parenchymal proliferating cells, whose phenotypical characterization remains largely unexplored. In the present study, we aimed to characterize the cortical grey matter proliferating cells during postnatal development, providing their stereological quantification and identifying the nature of their cell lineage. The number of grey matter proliferating cells (identified by means of Ki67 marker; Scholzen and Gerdes 2000; Kee et al. 2002; Taupin 2007) was estimated at different developmental stages, using the stereological optical fractionator method. Furthermore, we used different cell-type specific immunohistochemical markers to assess their cell lineage **focusing the quantitative analysis on the principal types of macroglial cells (astrocytes and oligodendrocytes).**

MATERIAL AND METHODS

Animals and tissue processing

A total of twenty-two **male** Sprague Dawley rats aged 2, 4, 7, 10, 14 and 21 days (three/four per age group) were analysed in this study. Rats, anesthetized with 10 mg/Kg Zoletil and 10 mg/Kg Xylazin, were transcardially perfused with 4% paraformaldehyde (PFA) in 0.1 M phosphate buffer (PB), **pH 7.2**, by means of a peristaltic pump. The brains were removed from the skull, immersed in 4% PFA in PB for 1day, cut into 50-μm-thick serial coronal sections by means of a vibratome VT1000S (Leica, Heidelberg, Germany), stored in PB and processed for immunohistochemistry.

Ki67 immunohistochemistry and stereological estimation of the total number of Ki67 labelled cells

Selected free-floating vibratome sections at different rostro-caudal levels were immunolabeled with an antibody against Ki67 (1:1000; Thermo Scientific, Rockford, IL, USA), according to a standard immunoperoxidase protocol (Moroni et al. 2013). For cytoarchitectural analysis, sections were counterstained with Cresyl Violet. Each stained section was digitized with a slice scanner (ScanScope; Aperio Technologies, Vista, CA, U.S.A.).

To determine the total number of Ki67-labelled cells in the entire rat neocortex of one hemisphere, an unbiased stereology protocol was employed, using a computer station with stereological software (Stereoinvestigator software, MicroBright-Field Inc, Colchester, Vermont, USA) consisting of a Leica DMLB microscope coupled to a Retiga 2000R colour uncooled camera and a motorized specimen stage. We first traced the grey matter neocortical profile on one hemisphere of each section using a 4x magnification. Counts were conducted at 40x. Based on a pilot study, every 20th section was sampled (the first section was selected randomly), with a sampling grid area of 122,500 μm^2 (for P2, P4, P7, and P10) and of 250,000 μm^2 (for P14 and P21), and a counting frame area of 6,400 μm^2 (for P2, P4, and P7), 8,100 μm^2 (for P10) and 19,600 μm^2 (for 14 and P21). The final measured section thickness was ~ 30 μm in the Z-axis. The Ki67 labelled cells were counted only as they came into focus within the counting frame area or touching or crossing an inclusion line (Fig. 1c). The total number of Ki67 labelled cells were evaluated with optical fractionators (Stereoinvestigator) and determined as the estimated population using mean section thickness (Table 2). The precision of the estimate of the total cell number in each subject was estimated as the coefficient of error (CE). The sampling was considered optimal when CE < 0.05.

Cell density was calculated as the ratio between total cell number and the estimated total volume. All counting data were expressed as means ± SEM.

Double immunofluorescence (IF) and cell counting

To characterize neocortical Ki67$^+$ cells, double immunofluorescence labelling with glial and neuronal markers was performed as described previously (Moroni et al. 2013). For a comprehensive list of the antibodies and their details, see Table 1. For double IF with antibodies raised in the same species (Ki67/Cux1), Fluorescein Tyramide Signal Amplification (TSA) Plus system (PerkinElmer Inc., Waltham, MA, USA) was used, following manufacture's instruction. Sections were counterstained with 4',6-diamidino-2-phenylindole (DAPI) (Molecular Probes), mounted with Fluorsave (Calbiochem, San Diego, CA, USA), and examined through a confocal microscope D-Eclipse C1 (Nikon, Tokyo, Japan) mounted on a light microscope Eclipse TE2000-E (Nikon). Confocal images were imported into Adobe Photoshop CS5 (Adobe Systems Incorporated, San Jose, CA, USA). Montages of images were constructed after adjustment of contrast and brightness. **Our quantitative analysis (Table 2) targeted proliferating cells double labeled with three glial markers: S100, NG2 and Olig2.** Cell counting was performed on acquired images taken at 40x magnification from two sections per rat by means of Image Pro-Plus 6.3 software (Media Cybernetics, MD, U.S.A.). Six (for P2-P10) or twelve (for P14 and P21) 318.3-μm-wide ROIs were randomly positioned within **the somatosensory cortex**. Double labelled cells were counted and their percentages among Ki67$^+$ cells were calculated (Table 2). To estimate the number of S100β$^+$, Olig2$^+$ or NG2$^+$ proliferating cells **we calculated the percentage, obtained by cell counting of double labelled cells (Ki67$^+$/S100β$^+$, Ki67$^+$/NG2$^+$ and Ki67$^+$/Olig2$^+$), of the number of proliferating cell at each age, estimated with the optical fractionator (Fig.6).**

Double fluorescent labelling with in situ Hybridization (ISH) and IF

In order to implement the panel of neuronal marker for proliferating cell characterization, double ISH and IF were carried out using the DIG-labelled riboprobe for *Er81*, marker of pyramidal layer V neurons (Watakabe et al., 2007), and anti-Ki67 antibody. ISH protocol was described previously (Moroni et al. 2009). After hybridization, the sections were incubated with mouse anti-DIG (1:50000; Sigma) and anti-Ki67 antibodies and visualized with Cy3–conjugated goat anti-mouse IgG (1:600; Jackson) and streptavidin–horseradish peroxidase (HRP) (PerkinElmer, Boston, USA) respectively.

Statistical analysis

The trend of the density, the estimated number of proliferating cells, and the percentage of **Ki67$^+$** cells double labelled with glial markers was investigated computing the best fitting quadratic curve.

This model allows to highlight both monophasic trends of increase or reduction as well as biphasic trends with the presence of peaks or nadirs. **All data sets were tested for normal distribution using the Shapiro-Wilk test and analyzed using a parametric statistics.** Proliferating cells expressing Olig2 and NG2 **were compared using a paired t-test. A Bonferroni correction was applied and a p<0.008 was considered significant.** The estimated number of double labelled Ki67$^+$ cells were expressed as mean ± standard error and compared **at each time point using a repeated measures ANOVA. We used a Greenhouse-Geisser correction when the Mauchly's test demonstrated a lack of sphericity. A Bonferroni correction was applied and a p<0.008 was considered significant. A post-hoc comparison in significant time-point was performed using a paired t-test. After Bonferroni correction for multiple comparison, a p<0.017 was considered significant.** IBM SPSS Statistics for Macintosh Version 25.0 (Armonk, NY, U.S.A.) was used to perform all the analyses.

RESULTS

Quantification of Ki67$^+$ proliferating cells

To identify the proliferating cells of the rat cerebral neocortex during postnatal development, we used the Ki67 protein as proliferation marker. Ki67$^+$ cells were distributed in all cortical layers (Fig. 1a). Three-dimensional cell counting revealed a monophasic reduction of Ki67$^+$ cell density (quadratic best fitting curve $r^2 = 0.87$, $p < 0.01$) from P2 (30,079 ± 951 cell/mm^3) to P21 (1848 ± 136 cell/ mm^3) (Fig. 1b).

To overcome bias due to changes in brain volume and cell density, which are significant during development, we applied the optical fractionator to estimate the total number of Ki67$^+$ cells in the grey matter of the entire cerebral hemicortex (Fig. 1c). This further analysis showed a biphasic trend of Ki67$^+$ cell number (quadratic best fitting curve $r^2 = 0.71$, $p < 0.01$): it increased during the first week of life, **peaking** between P7 **and** P10 (1.47 x 10^6 ± 0.26 x 10^6 at P7; 1.18 x 10^6 ± 0.11 x 10^6 at P10), and subsequently decreased until P21 (0.28 ± 0.02 x 10^6, Fig. 1d).

Immunohistochemical characterization of Ki67$^+$ proliferating cells

In order to characterize the cell lineage of the grey matter proliferating cells, we performed double IF combining Ki67 antibody with a panel of fourteen markers labelling astrocytes, oligodendrocytes

or neurons (Table 1). To **quantify** different type of proliferating cells, we estimated the proportion of S100$^+$, Olig2$^+$ or NG2$^+$ **glial** cells among the Ki67$^+$ cells.

Astrocyte markers: S100β, Aldh1L1, GLAST, and GFAP

We used S100β as astrocyte marker (Fig. 2a-e). Quantitative double IF evaluation revealed that the percentage of proliferating cells **expressing** S100β had a biphasic trend (quadratic best fitting curve $r^2 = 0.54$, p = 0.01): a very slight increase until P4-10 (range between **20.16 ± 9.91%** and **22.77 ± 10.08%**) and subsequently a reduction until P21, when the percentage of Ki67$^+$/S100β$^+$ cells was negligible (**0.35 ± 0.70%**; Fig. 2f).

Although S100β is primarily considered an astrocytic protein (Sen and Belli 2007; Patro et al. 2015), its immunodetection has also been reported in oligodendrocytes during development or rarely in neurons (Rickmann and Wolff 1995; Hachem et al. 2005). To overcome this debate, we analysed additional astrocyte markers: Aldh1L1, GLAST, and GFAP. Double IF showed that Aldh1L1 co-localised almost totally with S100β (Fig. 3a, b) and the percentage trend of the Aldh1L1$^+$ proliferating cells overlapped with that of S100β (Fig. 3c). The qualitative analyses of GLAST and GFAP revealed that they were expressed in Ki67$^+$ cells (Fig. 3d, e, g, h) and co-localised with S100β (Fig. 3f, i). Moreover, S100β was not expressed in cells positive for NeuN (Fig. S1a), considered to be a specific neuronal marker (Gusel'nikova and Korzhevskiy 2015) **nor for doublecortin (Fig. S1b, c), marker of migrating neurons (Francis et al. 1999; Gleeson et al. 1999).**

Oligodendrocyte markers: Olig2 and NG2

We used Olig2 as **oligodendrocytes** marker (Fig. 4a-c). The percentage of proliferating cells expressing Olig2 showed a biphasic trend (quadratic best fitting curve $r^2 = 0.93$, p < 0.001): it decreased during the first postnatal week (range between **57.32 ± 4.63%** and **30.95 ± 5.14%**), reaching the minimum at P7-P10 and subsequently increased until P21 (**86.40 ± 2.77%**) (Fig. 4g). Because it has been reported that Olig2 is transiently expressed in immature astrocytes during neonatal stages (Cai et al. 2007; Ono et al. 2008), we analysed as second oligodendrocyte marker NG2, used to identify oligodendrocyte precursor cells (OPCs) in both developing and adult brain (Fig. 4d-f). The Ki67$^+$/NG2$^+$ cell number ratio was almost constant during the first postnatal week and subsequently augmented, reaching the peak at P21 (**82.53 ± 5.50%**, Fig. 4g) (quadratic best fitting curve $r^2 = 0.95$, p < 0.001).

Comparing the percentage trends of Olig2$^+$ and NG2$^+$ proliferating cells, we noticed that they were overlapping with the exception of the first postnatal week, when the percentage of Ki67$^+$/Olig2$^+$ cells was larger than that of Ki67$^+$/NG2$^+$ cells (Fig. 4g). Interestingly, double IF revealed that

S100β and Olig2 co-localised during the first postnatal week, while double labelled cells were hardly found in the following two weeks (Fig. 5a-c). Moreover, **Olig2 and NG2** co-localised almost **completely** from the second postnatal week onwards, while Olig2$^+$/NG2$^-$ cells were detectable during the first postnatal week (Fig. 5d-f).

Considering the estimated number of S100β$^+$ proliferating cells, we confirmed that they showed a biphasic trend (best fitting quadratic curve $r^2 = 0.51$, $p = 0.01$), with an increase till P7/P10 and then a decrease till P21, when there were virtually no S100β$^+$ proliferating cells (Fig. 6). Even if the percentage of Olig2$^+$ and NG2$^+$ proliferating cells showed an increase of both cell lineages at the end of the third postnatal week (P21) (Fig. 4**g**), the estimated number of Olig2$^+$and NG2$^+$ proliferating cells was almost **constant** during the first two postnatal weeks and then showed a reduction **trend** at P21 (Fig. 6). The overall comparison of the three markers revealed that Olig2$^+$ and NG2$^+$ proliferating cells were more numerous than **S100β** $^+$ proliferating cells **from** P14. Moreover, it confirmed that Ki67$^+$/Olig2$^+$ cells were more numerous than Ki67$^+$/NG2$^+$ cells at P2 and P4, whereas they showed no significant differences from P7 onwards (paired t-test, $p < 0.05$).

Neuronal, endothelial, and microglial markers

With the aim to investigate the nature of the proliferating cells not **expressing** the employed glial markers, we performed double IF or *in situ* hybridization with Ki67 antibody and the following markers: NeuN (marker of mature neurons - Fig. S1**d**), GAD67, calbindin, calretinin (markers of **precursor and mature** GABAergic neurons - Fig. S1**e-g**), **doublecortin (marker of migrating neurons – Fig. S1h, i)**, Cux-1, and ER81 (markers of **precursor and mature** glutamatergic neurons - Fig. S1**j, k**). No double labelled cells were detected with the tested antibodies in the cortical grey matter, **whereas** double labelled cells were **observed** in the cortical SVZ (data not shown). Conversely, double IF for Ki67 and either CD31(Newman et al. 1990) or tomato lectin (Dalmau et al. 2003) revealed that some proliferating cells belonged to endothelial and microglial cell lineage respectively (Fig. S2).

DISCUSSION

While progenitors of VZ/SVZ have been the focus of many studies, still little is known about progenitors of the CNS parenchyma, despite their widespread nature. Neural progenitor cells have been found outside the main germinative zones in both embryonic and adult cerebral cortex (Dawson et al. 2003; Costa et al. 2007; Dimou et al. 2008), but their specific characterization during postnatal development is lacking. The postnatal **brain** development is characterized by a substantial

increase in weight and size (Duffell et al. 2000; Bandeira et al. 2009; Seelke et al. 2012), ascribed to increasing neuronal size, branching and pruning of the dendritic trees, and a massive addition of glial cells or even neurons (Lyck et al. 2007; Bandeira et al. 2009). This occurs concomitantly to the shrinkage of VZ and SVZ, suggesting the existence of other germinative niches **in the postnatal cortex**. Hence, the importance of grey matter proliferating cells and the need of studying their nature.

To identify proliferating cells, we used the Ki67 protein because it is expressed during all active phases of the cell cycle, while is down-regulated in resting (G_0) cells (Scholzen and Gerdes 2000; Taupin 2007). Ki67 protein allows a better estimation of the proliferating activity if compared to markers, such **as** the proliferating nuclear antigen (PCNA) or BrdU, markers of S-phase (Zolzer et al. 2010) or DNA synthesis, respectively. We used a stereological method for the unbiased quantification of the proliferating cells of the entire hemicortex, during rat postnatal development. The results showed that the total number of proliferating cells increase during the first postnatal week **until P10** and decrease during the following weeks **until P21**. This seems to be in contrast with the calculated density of proliferating cells, **that progressively decrease in number** from P2 to P21. This difference is explained by the massive growth of the neocortex occurring during development, which implicates volume and mass increase, cell number gain but also cell density decrease. The optical fractionator, considered to be insensitive to volume changes, cell sizes and cell density (Dorph-Petersen et al. 2001; Schmitz and Hof 2005; Lyck et al. 2007) was applied to overcome bias from these sources and our data showed that stereology provides a better approach for quantifying cell populations during brain development. The increment of proliferating cells observed **before** P10 occurs concomitantly to the shrinkage of SVZ, considered to be an essential source of glial cells (Burns et al. 2009). Thus, our data are consistent with the idea that, during development, grey matter represents an important source of new born cells.

In order to characterize the cell lineages of the grey matter proliferating cells, we performed double IF combining Ki67 protein with different markers of astrocytes, oligodendrocytes or neurons. The selection of specific cell lineage markers presents a tricky task, because of the overlapping expression of some proteins in the same lineage during development or the lack of cell lineage characterization. This is the case of astrocytes: although they are essential in CNS physiology, their molecular identity remains largely uncharacterized, partially due to the lack of reliable markers apt to investigate their functional and morphological heterogeneity (Rowitch and Kriegstein 2010; Bayraktar et al. 2014; Molofsky and Deneen 2015; Tabata 2015). To identify astrocytes we chose the calcium binding protein S100β because, in both early postnatal stages and adulthood, it is expressed in the cell body, allowing the precise identification of the cells (Savchenko et al. 2000;

9

Patro et al. 2015). Although its immunodetection has also been reported in oligodendrocytes **and** rarely in neurons (Rickmann and Wolff 1995; Hachem et al. 2005), we demonstrated that S100β is a specific astrocyte marker in the cortical grey matter. Indeed, we showed that S100β$^+$ cells co-express the aldehyde dehydrogenase 1 family member L1 (Aldh1L1), the glutamate-aspartate transporter (GLAST), and the glial fibrillary acidic protein (GFAP), all considered to be specific astrocyte markers (Lehre et al. 1995; Williams et al. 2005; Cahoy et al. 2008; Sofroniew and Vinters 2010; Molofsky et al. 2013; Molofsky and Deneen 2015); **these markers** are primarily distributed **in** astroglial processes, thus being less suitable to clearly identify individual astrocytes. Moreover, we found that S100β was not expressed in cells positive for the neuronal markers NeuN, **nor DCX**, thus excluding its expression in neurons**.** To identify oligodendrocytes, we chose the transcription factor Olig2, which is expressed in cell nuclei throughout the oligodendrocyte lineage, including the mature oligodendrocytes (Ligon et al. 2006; Kessaris et al. 2008; Geha et al. 2010). As it has been shown that Olig2$^+$ progenitor cells change their differentiative properties during development and could have a role also in astrocyte development (Cai et al. 2007; Ono et al. 2008), we decided to analyse also the chondroitin sulfate proteoglycan NG2. This is expressed in the oligodendrocyte precursor cells (OPCs), **and** it is absent in neurons (Karram et al. 2008; Clarke et al. 2012) and astrocytes, at least in the dorsal cortex (Zhu et al. 2008; Nobs et al. 2014; Huang et al. 2016). **This makes NG2** a good oligodendrocyte lineage marker, although **in the rat its labelling is more faint than in other species (i.e. mouse and human)**, rendering cell identification **more** difficult. The percentages of Olig2$^+$ and NG2$^+$ proliferating cells were overlapping, with the exception of the first postnatal week, when the former overtook the latter. This **suggests** that, during the first postnatal week, Olig2 is expressed in cells other than OPCs, most likely in astrocytes. Indeed, it has been reported that Olig2 is transiently expressed in immature astrocytes at early postnatal stages (Cai et al. 2007; Ono et al. 2008), and we found that S100β and Olig2 co-localised during the first postnatal week, while double labelled cells were hardly found in the following two weeks. In summary, Olig2 is a better oligodendrocyte marker than NG2 because of its nuclear localisation, but during the first postnatal week it is not exclusively expressed by oligodendrocytes. The canonical view of cortical development states that cortical progenitor cells pursue temporal yet overlapping waves of development, with neurons generating first, during the embryonic life, followed by astrocytes, during the first postnatal week, and subsequently oligodendrocytes, during the second postnatal week (Sauvageot and Stiles 2002; Miller and Gauthier 2007). However, previous experimental data on progenitor cell development were mostly generated by retroviral lineage-tracing of VZ and SVZ progenitors. Recent studies suggested a new scenario. Bandeira and co-authors showed that in most rat brain structures, including the cerebral cortex, the neuronal

population has a net increase between P3 and P7, followed by a net loss between P7 and P15, concurrent with the generation of the glial population (Bandeira et al. 2009). This implies that there is neurogenesis during the first postnatal week and gliogenesis during the second. Consistently with the hypothesis of the SVZ origin of new-born neurons during the first postnatal week (Bandeira et al. 2009), we found neuronal proliferating cells in SVZ but not in the cortical grey matter. In agreement with Ge and co-authors (2012), who stated that a major source of glia in the mouse postnatal cortex is the local proliferation of differentiated astrocytes, we found proliferating astrocytes in the cortical grey matter. These cells ranged between 10-20% of the proliferating cells **before** P10 and progressively decreased, until disappearing at the end of the third postnatal week. Our findings confirm that astrogliogenesis occurs prevalently during the first 10 days of postnatal development, as previously reported in a genetic fate-mapping study demonstrating that cortical astrocytes quickly exhaust their proliferation capacity by P10 (Burns et al. 2009). This seems to be in contradiction with **previous** data obtained using isotropic fractionator that showed an increased number of non-neuronal cells (thus glial cells) in the second postnatal week (Bandeira et al. 2009). However, **these** authors made a gross distinction between neuronal and non-neuronal cells, not distinguishing between astrocytes, oligodendrocytes and microglia, which are heavily generated during the second postnatal week.

We found that the number of OPCs ($NG2^+/Ki67^+$ cells) tended to be higher than that of proliferating astrocytes in all the analysed ages (although not statistically significant) and, at P21, they represented the main proliferating cells of the cortical grey matter (Fig.6). According to literature, oligodendrocyte proliferation would be expected from the second postnatal week onwards. Indeed, a peak of oligodendrogenesis was found during the second postnatal week (Sauvageot and Stiles 2002) and it has been shown that OPCs are the major dividing cell population of the adult rat CNS (Dawson et al. 2003; Mori et al. 2009; Nobs et al. 2014). Thus, the high number of OPCs during the first postnatal week was unexpected; moreover, **their temporal distribution revealed the presence of** a permanent pool enduring in the postnatal cortical grey matter since birth. **Although we cannot distinguish locally generated oligodendrocytes from those cells that still may migrate into the cortex from other sources (Kessaris te al., 2006)**, we speculate that OPCs **could** migrate to the grey matter before the disappearance of radial glia and **before** the arrival of axons from callosal projection neurons that pass through the white matter after birth and likely form a physical barrier to precursor migration. **The involution of radial glia (Misson et al. 1991; Stichel et al. 1991) and the formation of callosal projections (Wang et al. 2007) occur within the first two postnatal weeks.** Thus, OPCs would reach their final position after birth, **giving rise to** grey matter oligodendrocytes. The peak of oligodendrogenesis described

during the second postnatal week **could** probably give birth to white matter oligodendrocytes **(Levison et al. 1993). However, to support this assumption, further experiments are mandatory.**

From our data, we can infer that, during the first two postnatal weeks, a percentage of proliferating cells did not express any of the analysed astrocyte or oligodendrocyte markers. To reveal the nature of these cells we tested a panel of markers apt to identify both excitatory and inhibitory neurons: no double labelled **neuronal** cells were detected in grey matter. These proliferating cells could **either** belong to astrocyte or oligodendrocyte subpopulations not **identified** by the used marker or, more probably, they may be endothelial or microglial cells. In fact, both endothelial and microglial cell proliferation has been documented in developing brain (Dalmau et al. 2003; Harb et al. 2013) and **was** confirmed **in** our **study by the** double labelling experiments showing both CD31^{+} and tomato lectin^{+} proliferating cells.

In conclusion, this study provides novel evidence on the extent of proliferative cells in cortical grey matter and on their phenotypic characterization during postnatal development. We showed that proliferating cells underwent an increase until P10 and decreased during the following two weeks. Furthermore, cell lineage characterization revealed a short period of cortical grey matter astrocyte proliferation in contrast to the endurance of oligodendrocyte proliferation from birth to adulthood. It is to be hoped that this study will help to reinterpret previous data about cortical gliogenesis, **in light of the relevance of glial proliferation within the grey matter**, and it will be a point of departure for further investigations of this complex process.

EHICAL APPROVAL

All the experiments were performed in accordance with the guidelines defined by the European Communities Council Directive (2010/63/EU) and the experimental protocol was approved by the Ethics Committee of the Italian Ministry of Health (authorization number 143-2016-PR). All efforts were made to limit the number of animals used and their suffering.

REFERENCES

Bandeira F, Lent R, Herculano-Houzel S (2009) Changing numbers of neuronal and non-neuronal cells underlie postnatal brain growth in the rat. Proc Natl Acad Sci U S A 106:14108-14113. doi: 10.1073/pnas.0804650106 [doi]

Bayer SA, Altman J, Russo RJ, Zhang X (1993) Timetables of neurogenesis in the human brain based on experimentally determined patterns in the rat. Neurotoxicology 14:83-144

Bayraktar OA, Fuentealba LC, Alvarez-Buylla A, Rowitch DH (2014) Astrocyte development and heterogeneity. Cold Spring Harb Perspect Biol 7:a020362. doi: 10.1101/cshperspect.a020362 [doi]

Burns KA, Murphy B, Danzer SC, Kuan CY (2009) Developmental and post-injury cortical gliogenesis: a genetic fate-mapping study with Nestin-CreER mice. Glia 57:1115-1129. doi: 10.1002/glia.20835 [doi]

Cahoy JD, Emery B, Kaushal A, Foo LC, Zamanian JL, Christopherson KS, Xing Y, Lubischer JL, Krieg PA, Krupenko SA et al (2008) A transcriptome database for astrocytes, neurons, and oligodendrocytes: a new resource for understanding brain development and function. J Neurosci 28:264-278. doi: 10.1523/JNEUROSCI.4178-07.2008 [doi]

Cai J, Chen Y, Cai WH, Hurlock EC, Wu H, Kernie SG, Parada LF, Lu QR (2007) A crucial role for Olig2 in white matter astrocyte development. Development 134:1887-1899. doi: dev.02847 [pii]

Celio MR, Baier W, Scharer L, Gregersen HJ, de Viragh PA, Norman AW (1990) Monoclonal antibodies directed against the calcium binding protein Calbindin D-28k. Cell Calcium 11:599-602. doi: 0143-4160(90)90014-L [pii]

Clarke LE, Young KM, Hamilton NB, Li H, Richardson WD, Attwell D (2012) Properties and fate of oligodendrocyte progenitor cells in the corpus callosum, motor cortex, and piriform cortex of the mouse. J Neurosci 32:8173-8185. doi: 10.1523/JNEUROSCI.0928-12.2012 [doi]

Costa MR, Kessaris N, Richardson WD, Gotz M, Hedin-Pereira C (2007) The marginal zone/layer I as a novel niche for neurogenesis and gliogenesis in developing cerebral cortex. J Neurosci 27:11376-11388. doi: 27/42/11376 [pii]

Dalmau I, Vela JM, Gonzalez B, Finsen B, Castellano B (2003) Dynamics of microglia in the developing rat brain. J Comp Neurol 458:144-157. doi: 10.1002/cne.10572

Dawson MR, Polito A, Levine JM, Reynolds R (2003) NG2-expressing glial progenitor cells: an abundant and widespread population of cycling cells in the adult rat CNS. Mol Cell Neurosci 24:476-488. doi: S1044743103002100 [pii]

Dimou L, Simon C, Kirchhoff F, Takebayashi H, Gotz M (2008) Progeny of Olig2-expressing progenitors in the gray and white matter of the adult mouse cerebral cortex. J Neurosci 28:10434-10442. doi: 10.1523/JNEUROSCI.2831-08.2008 [doi]

Dorph-Petersen KA, Nyengaard JR, Gundersen HJ (2001) Tissue shrinkage and unbiased stereological estimation of particle number and size. J Microsc 204:232-246. doi: 958 [pii]

Duffell SJ, Soames AR, Gunby S (2000) Morphometric analysis of the developing rat brain. Toxicol Pathol 28:157-163. doi: 10.1177/019262330002800120 [doi]

Francis F, Koulakoff A, Boucher D, Chafey P, Schaar B, Vinet M, Friocourt G, McDonnel N, Reiner O, Kahn A, McConnell SK, Berwald-Netter Y, Denoulet P, Chelly J (1999) Doublecortin is a developmentally regulated, microtubule-associated protein expressed in migrating and differentiating neurons. Neuron 23:247-256

Franco SJ, Muller U (2013) Shaping our minds: stem and progenitor cell diversity in the mammalian neocortex. Neuron 77:19-34. doi: 10.1016/j.neuron.2012.12.022 [doi]

Ge WP, Jia JM (2016) Local production of astrocytes in the cerebral cortex. Neuroscience 323:3-9. doi: 10.1016/j.neuroscience.2015.08.057 [doi]

Ge WP, Miyawaki A, Gage FH, Jan YN, Jan LY (2012) Local generation of glia is a major astrocyte source in postnatal cortex. Nature 484:376-380. doi: 10.1038/nature10959 [doi]

Geha S, Pallud J, Junier MP, Devaux B, Leonard N, Chassoux F, Chneiweiss H, Daumas-Duport C, Varlet P (2010) NG2+/Olig2+ cells are the major cycle-related cell population of the adult human normal brain. Brain Pathol 20:399-411. doi: 10.1111/j.1750-3639.2009.00295.x [doi]

Gleeson JG, Lin PT, Flanagan LA, Walsh CA (1999) Doublecortin is a microtubule-associated protein and is expressed widely by migrating neurons. Neuron 23:257-271

Gusel'nikova VV, Korzhevskiy DE (2015) NeuN As a Neuronal Nuclear Antigen and Neuron Differentiation Marker. Acta Naturae 7:42-47

Hachem S, Aguirre A, Vives V, Marks A, Gallo V, Legraverend C (2005) Spatial and temporal expression of S100B in cells of oligodendrocyte lineage. Glia 51:81-97. doi: 10.1002/glia.20184 [doi]

Harb R, Whiteus C, Freitas C, Grutzendler J (2013) In vivo imaging of cerebral microvascular plasticity from birth to death. J Cereb Blood Flow Metab 33:146-156. doi: 10.1038/jcbfm.2012.152 [doi]

Hevner RF (2006) From radial glia to pyramidal-projection neuron: transcription factor cascades in cerebral cortex development. Mol Neurobiol 33:33-50. doi: MN:33:1:033 [pii]

Huang Z, Sun D, Hu JX, Tang FL, Lee DH, Wang Y, Hu G, Zhu XJ, Zhou J, Mei L et al (2016) Neogenin Promotes BMP2 Activation of YAP and Smad1 and Enhances Astrocytic Differentiation in Developing Mouse Neocortex. J Neurosci 36:5833-5849. doi: 10.1523/JNEUROSCI.4487-15.2016 [doi]

Jacobowitz DM, Winsky L (1991) Immunocytochemical localization of calretinin in the forebrain of the rat. J Comp Neurol 304:198-218. doi: 10.1002/cne.903040205 [doi]

Karram K, Goebbels S, Schwab M, Jennissen K, Seifert G, Steinhauser C, Nave KA, Trotter J (2008) NG2-expressing cells in the nervous system revealed by the NG2-EYFP-knockin mouse. Genesis 46:743-757. doi: 10.1002/dvg.20440 [doi]

Kee N, Sivalingam S, Boonstra R, Wojtowicz JM (2002) The utility of Ki-67 and BrdU as proliferative markers of adult neurogenesis. J Neurosci Methods 115:97-105. doi: S0165027002000079 [pii]

Kessaris N, Fogarty M, Iannarelli P, Grist M, Wegner M, Richardson WD (2006) Competing waves of oligodendrocytes in the forebrain and postnatal elimination of an embryonic lineage. Nature Neuroscience 9:173-179. doi: 10.1038/nn1620

Kessaris N, Pringle N, Richardson WD (2008) Specification of CNS glia from neural stem cells in the embryonic neuroepithelium. Philos Trans R Soc Lond B Biol Sci 363:71-85. doi: B4465N34207557L5 [pii]

Lehre KP, Levy LM, Ottersen OP, Storm-Mathisen J, Danbolt NC (1995) Differential expression of two glial glutamate transporters in the rat brain: quantitative and immunocytochemical observations. J Neurosci 15:1835-1853

Levison SW, Chuang C, Abramson BJ, Goldman JE (1993) The migrational patterns and developmental fates of glial precursors in the rat subventricular zone are temporally regulated. Development 119:611-622

Ligon KL, Fancy SP, Franklin RJ, Rowitch DH (2006) Olig gene function in CNS development and disease. Glia 54:1-10. doi: 10.1002/glia.20273 [doi]

Lin CS, Lu SM, Schmechel DE (1986) Glutamic acid decarboxylase and somatostatin immunoreactivities in rat visual cortex. J Comp Neurol 244:369-383. doi: 10.1002/cne.902440309 [doi]

Lyck L, Kroigard T, Finsen B (2007) Unbiased cell quantification reveals a continued increase in the number of neocortical neurones during early post-natal development in mice. Eur J Neurosci 26:1749-1764. doi: EJN5763 [pii]

Miller FD, Gauthier AS (2007) Timing is everything: making neurons versus glia in the developing cortex. Neuron 54:357-369. doi: S0896-6273(07)00298-X [pii]

Misson JP, Takahashi T, Caviness VS Jr (1991) Ontogeny of radial and other astroglial cells in murine cerebral cortex. Glia 4:138-148

Molofsky AV, Deneen B (2015) Astrocyte development: A Guide for the Perplexed. Glia 63:1320-1329. doi: 10.1002/glia.22836 [doi]

Molofsky AV, Glasgow SM, Chaboub LS, Tsai HH, Murnen AT, Kelley KW, Fancy SP, Yuen TJ, Madireddy L, Baranzini S et al (2013) Expression profiling of Aldh1l1-precursors in the developing spinal cord reveals glial lineage-specific genes and direct Sox9-Nfe2l1 interactions. Glia 61:1518-1532. doi: 10.1002/glia.22538 [doi]

Mori T, Wakabayashi T, Takamori Y, Kitaya K, Yamada H (2009) Phenotype analysis and quantification of proliferating cells in the cortical gray matter of the adult rat. Acta Histochem Cytochem 42:1-8. doi: 10.1267/ahc.08037 [doi]

Moroni RF, Inverardi F, Regondi MC, Pennacchio P, Spreafico R, Frassoni C (2013) Genesis of heterotopia in BCNU model of cortical dysplasia, detected by means of in utero electroporation. Dev Neurosci 35:516-526. doi: 10.1159/000355392 [doi]

Moroni RF, Inverardi F, Regondi MC, Watakabe A, Yamamori T, Spreafico R, Frassoni C (2009) Expression of layer-specific markers in the adult neocortex of BCNU-Treated rat, a model of cortical dysplasia. Neuroscience 159:682-691. doi: 10.1016/j.neuroscience.2008.12.064

Newman PJ, Berndt MC, Gorski J, White GC,2nd, Lyman S, Paddock C, Muller WA (1990) PECAM-1 (CD31) cloning and relation to adhesion molecules of the immunoglobulin gene superfamily. Science 247:1219-1222

Nieto M, Monuki ES, Tang H, Imitola J, Haubst N, Khoury SJ, Cunningham J, Gotz M, Walsh CA (2004) Expression of Cux-1 and Cux-2 in the subventricular zone and upper layers II-IV of the cerebral cortex. J Comp Neurol 479:168-180. doi: 10.1002/cne.20322 [doi]

Nobs L, Baranek C, Nestel S, Kulik A, Kapfhammer J, Nitsch C, Atanasoski S (2014) Stage-specific requirement for cyclin D1 in glial progenitor cells of the cerebral cortex. Glia 62:829-839. doi: 10.1002/glia.22646 [doi]

Noctor SC, Martinez-Cerdeno V, Ivic L, Kriegstein AR (2004) Cortical neurons arise in symmetric and asymmetric division zones and migrate through specific phases. Nat Neurosci 7:136-144. doi: 10.1038/nn1172 [doi]

Ono K, Takebayashi H, Ikeda K, Furusho M, Nishizawa T, Watanabe K, Ikenaka K (2008) Regional- and temporal-dependent changes in the differentiation of Olig2 progenitors in the forebrain, and the impact on astrocyte development in the dorsal pallium. Dev Biol 320:456-468. doi: 10.1016/j.ydbio.2008.06.001 [doi]

Parnavelas JG (2000) The origin and migration of cortical neurones: new vistas. Trends Neurosci 23:126-131. doi: S0166-2236(00)01553-8 [pii]

Parnavelas JG (1999) Glial cell lineages in the rat cerebral cortex. Exp Neurol 156:418-429. doi: S0014-4886(99)97044-9 [pii]

Patro N, Naik A, Patro IK (2015) Differential temporal expression of S100beta in developing rat brain. Front Cell Neurosci 9:87. doi: 10.3389/fncel.2015.00087 [doi]

Rickmann M, Wolff JR (1995) S100 protein expression in subpopulations of neurons of rat brain. Neuroscience 67:977-991. doi: 0306-4522(94)00615-C [pii]

Rowitch DH, Kriegstein AR (2010) Developmental genetics of vertebrate glial-cell specification. Nature 468:214-222. doi: 10.1038/nature09611 [doi]

Sanchez MP, Frassoni C, Alvarez-Bolado G, Spreafico R, Fairen A (1992) Distribution of calbindin and parvalbumin in the developing somatosensory cortex and its primordium in the rat: an immunocytochemical study. J Neurocytol 21:717-736

Sauvageot CM, Stiles CD (2002) Molecular mechanisms controlling cortical gliogenesis. Curr Opin Neurobiol 12:244-249. doi: S0959438802003227 [pii]

Savchenko VL, McKanna JA, Nikonenko IR, Skibo GG (2000) Microglia and astrocytes in the adult rat brain: comparative immunocytochemical analysis demonstrates the efficacy of lipocortin 1 immunoreactivity. Neuroscience 96:195-203. doi: S0306-4522(99)00538-2 [pii]

Schmitz C, Hof PR (2005) Design-based stereology in neuroscience. Neuroscience 130:813-831. doi: S0306-4522(04)00851-6 [pii]

Scholzen T, Gerdes J (2000) The Ki-67 protein: from the known and the unknown. J Cell Physiol 182:311-322. doi: 10.1002/(SICI)1097-4652(200003)182:3<311::AID-JCP1>3.0.CO;2-9 [pii]

Seelke AM, Dooley JC, Krubitzer LA (2012) The emergence of somatotopic maps of the body in S1 in rats: the correspondence between functional and anatomical organization. PLoS One 7:e32322. doi: 10.1371/journal.pone.0032322 [doi]

Sen J, Belli A (2007) S100B in neuropathologic states: the CRP of the brain? J Neurosci Res 85:1373-1380. doi: 10.1002/jnr.21211 [doi]

Sofroniew MV, Vinters HV (2010) Astrocytes: biology and pathology. Acta Neuropathol 119:7-35. doi: 10.1007/s00401-009-0619-8 [doi]

Spreafico R, De Biasi S, Frassoni C, Battaglia G (1988) A comparison of GAD- and GABA-immunoreactive neurons in the first somatosensory area (SI) of the rat cortex. Brain Res 474:192-196. doi: 0006-8993(88)90684-1 [pii]

Stichel CC, Müller CM, Zilles K (1991) Distribution of glial fibrillary acidic protein and vimentin immunoreactivity during rat visual cortex development. J Neurocytol 20(2):97-108

Tabata H (2015) Diverse subtypes of astrocytes and their development during corticogenesis. Front Neurosci 9:114. doi: 10.3389/fnins.2015.00114 [doi]

Taupin P (2007) BrdU immunohistochemistry for studying adult neurogenesis: paradigms, pitfalls, limitations, and validation. Brain Res Rev 53:198-214. doi: S0165-0173(06)00104-4 [pii]

Wang CL, Zhang L, Zhou Y, Zhou J, Yang XJ, Duan SM, Xiong ZQ, Ding YQ (2007) Activity-dependent development of callosal projections in the somatosensory cortex. J Neurosci 27:11334-11342. doi: 27/42/11334 [pii]

Watakabe A, Ichinohe N, Ohsawa S, Hashikawa T, Komatsu Y, Rockland KS, Yamamori T (2007) Comparative analysis of layer-specific genes in Mammalian neocortex. Cereb Cortex 17:1918-1933. doi: 10.1093/cercor/bhl102

Williams SM, Sullivan RK, Scott HL, Finkelstein DI, Colditz PB, Lingwood BE, Dodd PR, Pow DV (2005) Glial glutamate transporter expression patterns in brains from multiple mammalian species. Glia 49:520-541. doi: 10.1002/glia.20139 [doi]

Zhu X, Bergles DE, Nishiyama A (2008) NG2 cells generate both oligodendrocytes and gray matter astrocytes. Development 135:145-157. doi: dev.004895 [pii]

Zolzer F, Basu O, Devi PU, Mohanty SP, Streffer C (2010) Chromatin-bound PCNA as S-phase marker in mononuclear blood cells of patients with acute lymphoblastic leukaemia or multiple myeloma. Cell Prolif 43:579-583. doi: 10.1111/j.1365-2184.2010.00707.x [doi]

FIGURE CAPTIONS

Fig. 1 Quantification of the proliferating cells of the cerebral neocortical grey matter during postnatal development. **a** Details of the rat **somatosensory** cortex showing the reduction of Ki67 immunolabeling from P2 to P21; sections are counterstained with cresyl violet. **b** Graph showing the progressive reduction of Ki67$^+$ cell density with age ($r^2 = 0.87$, $p < 0.01$). **c** Series of frontal sections through the right cerebral hemisphere of a P7 rat showing the borders of the cortex analysed by means of optical fractionator. The detail shows the sampling grid area (dashed squares) and the counting frames (green lines represent the inclusion lines and red lines the exclusion lines); **d** Graph showing the biphasic trend of the estimated number of Ki67$^+$ cells that increases until P7-P10 and subsequently decreases until P21 ($r^2 = 0.71$, $p < 0.01$). Scale bars: **a** 160 μm; **c** 2.25 mm

Fig. 2 Representative confocal images of **the somatosensory cortex** showing double immunofluorescence for Ki67 (green) and S100β (red) at different postnatal ages. Ki67$^+$/S100β$^+$ cells are detectable at P2 (**a**) and P7 (**b**) (arrows in merge, arrowheads in single channels) but they are hardly detectable at P21 (**c**). **d** High magnification of a Ki67$^+$/S100β$^+$ dividing cell; nuclei are counterstained with DAPI. **e** Single plane image with orthogonal views showing an example of Ki67$^+$ cell expressing S100β. **f** Bar graph showing the percentage of S100β$^+$ proliferating cells during postnatal development ($r^2 = 0.54$, $p < 0.001$): note the slight increase until **P4-P10** and their disappearance at P21. Bar chart represents mean ± SEM. Scale bars: **a-c** 70.7 μm; **d** 10.6 μm; **e** 8.6μm

Fig. 3 Representative confocal images of **the somatosensory cortex** at different postnatal ages double labelled for different mixture of astrocytes markers. **a** Double immunofluorescence showing the complete co-localisation between S100β (green) and Aldh1L1 (red) proteins. **b** High magnification of the cell boxed in a. **c** Bar graph showing the percentage of Aldh1L1$^+$ proliferating cells ($r^2 = 0.55$, $p = 0.003$): note the similar trend of expression described for S100β$^+$ proliferating cells (fig.2). Bar chart represents mean ± SEM. **d** Ki67$^+$ cells expressing GLAST (arrows in merge, arrowheads in single channels). **e** High magnification of a Ki67$^+$/GLAST$^+$ dividing cell. **f** Co-localisation between S100β (green) and GLAST (red) proteins. **g** Ki67$^+$ cells expressing GFAP (arrows). **h** High magnification of a Ki67$^+$/GFAP$^+$ dividing cell. **i** Co-localisation between S100β (green) and GFAP (red) proteins. Scale bars: **a, d** 43 μm; **b, e** 21.5 μm; **f, i** 70.7 μm; **g** 62.9 μm; **h** 40.9 μm

Fig. 4 Representative confocal images of **the somatosensory cortex** showing double immunofluorescence for Ki67 (green) and Olig2 (red) (**a-c**) or NG2 (**d-f**). Examples of Ki67$^+$/Olig2$^+$ or Ki67$^+$/NG2$^+$ cells are indicated by arrows (merge images) or by arrowheads (single channel images). Inset in **c** high magnification of two Ki67$^+$/Olig2$^+$ cells. Insets in **e, f** high magnification of Ki67$^+$/NG2$^+$ proliferating cells. **g** Bar graph showing the comparison between Olig2$^+$ and NG2$^+$ proliferating cells: note the overlapping with the exception of P2 and P4, when the percentage of Ki67$^+$/Olig2$^+$ cells was larger than that of Ki67$^+$/NG2$^+$ cells (* $P < 0.05$). Bar charts represent mean ± SEM. Scale bars: **a-c, d-f** 70.7 μm; inset in c, **e**, and **f**: 40 μm

Fig. 5 Representative confocal images of **the somatosensory cortex** showing double immunofluorescence for Olig2 (green) and S100β (**a-c**) or NG2 (**d-f**) proteins (red) at different postnatal ages. Olig2$^+$/S100β$^+$ cells (arrows in merge and arrowheads in single channel) are prevalently detectable during the first postnatal week (**a, b**), while they are hardly detectable afterwards (**c**).Both Olig2$^+$/NG2$^-$ (arrowheads) and Olig2$^+$/NG2$^+$ (arrows) cells are detectable during the first postnatal week (**d**), while Olig2 and NG2 co-localise almost totally from the second postnatal week onwards (**e-f**). Scale bars: **a-e** 70.7 μm; inset in e: 42.5 μm; **f** 47 μm

Fig. 6 Comparison of the estimated number of S100β$^+$, Olig2$^+$ or NG2$^+$ proliferating cells. Note that astrocytes (S100β$^+$ cells) exhaust their proliferation capacity at the end of second postnatal weeks, whereas the number of proliferating oligodendrocytes (Olig2$^+$ or NG2$^+$ cells) is almost constant during all the analysed ages. Ki67$^+$/Olig2$^+$ cells were more numerous than Ki67$^+$/NG2$^+$ cells at P2 and P4, while they showed no significant differences from P7 onwards. Bar chart represents mean ± SEM (**$P < 0.01$)

Fig. S1 Representative confocal images of **the somatosensory cortex** at different postnatal ages double labelled for different mixture of neuronal markers. No co-localisation between S110β (green) and NeuN (red) (**a**) **nor doublecortin (DCX - red) (b, c)** proteins is detectable. The expression analysis of proliferating cells (Ki67$^+$, green) with the neuronal markers (red) NeuN (**d**), GAD67 (**e**), **calretinin (CR) (f)**, **calbindin (CB) (g)**, **DCX (h, i)**, Cux-1 (**j**), or ER81 (**k**) does not reveal any co-localisation. Scale bars: **a, d, e-g, j, k** 70.7 μm; **b, c, h** 55 μm; **i** 65 μm

Fig. S2 Representative confocal images of **the somatosensory cortex** at P7 double labelled for Ki67 and endothelial or microglial markers. **a, b** Details of vessels labelled with CD31 (red); proliferating (Ki67$^+$, green) endothelial cells are indicated with arrows. **c, d** Microglial cells labelled

with Tomato lectin (red); proliferating (Ki67$^+$, green) microglial cells are indicated with arrows. Scale bars: **a** 42.8 μm; **b** 16.5 μm; **c** 70.7 μm; **d** 31 μm
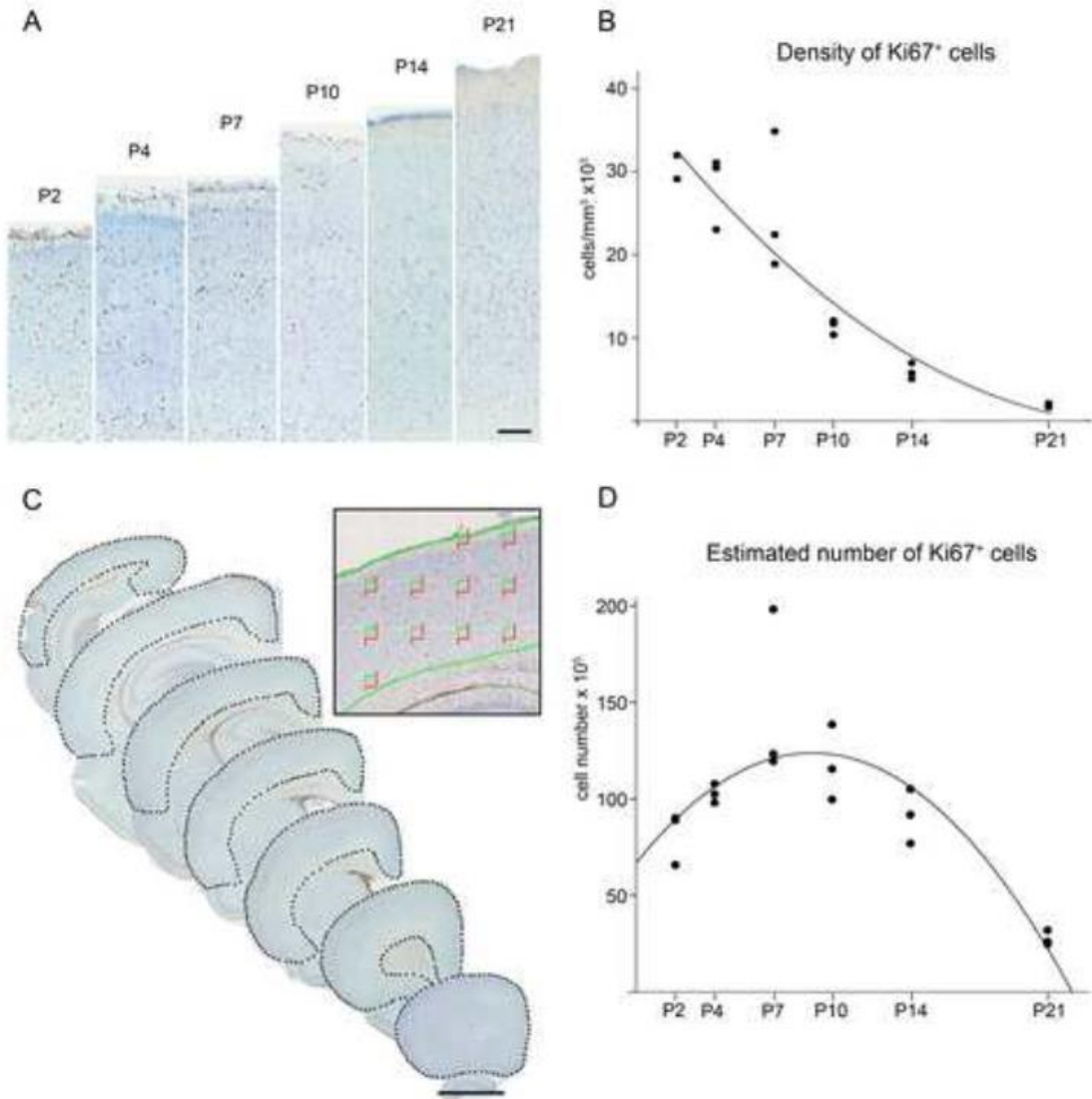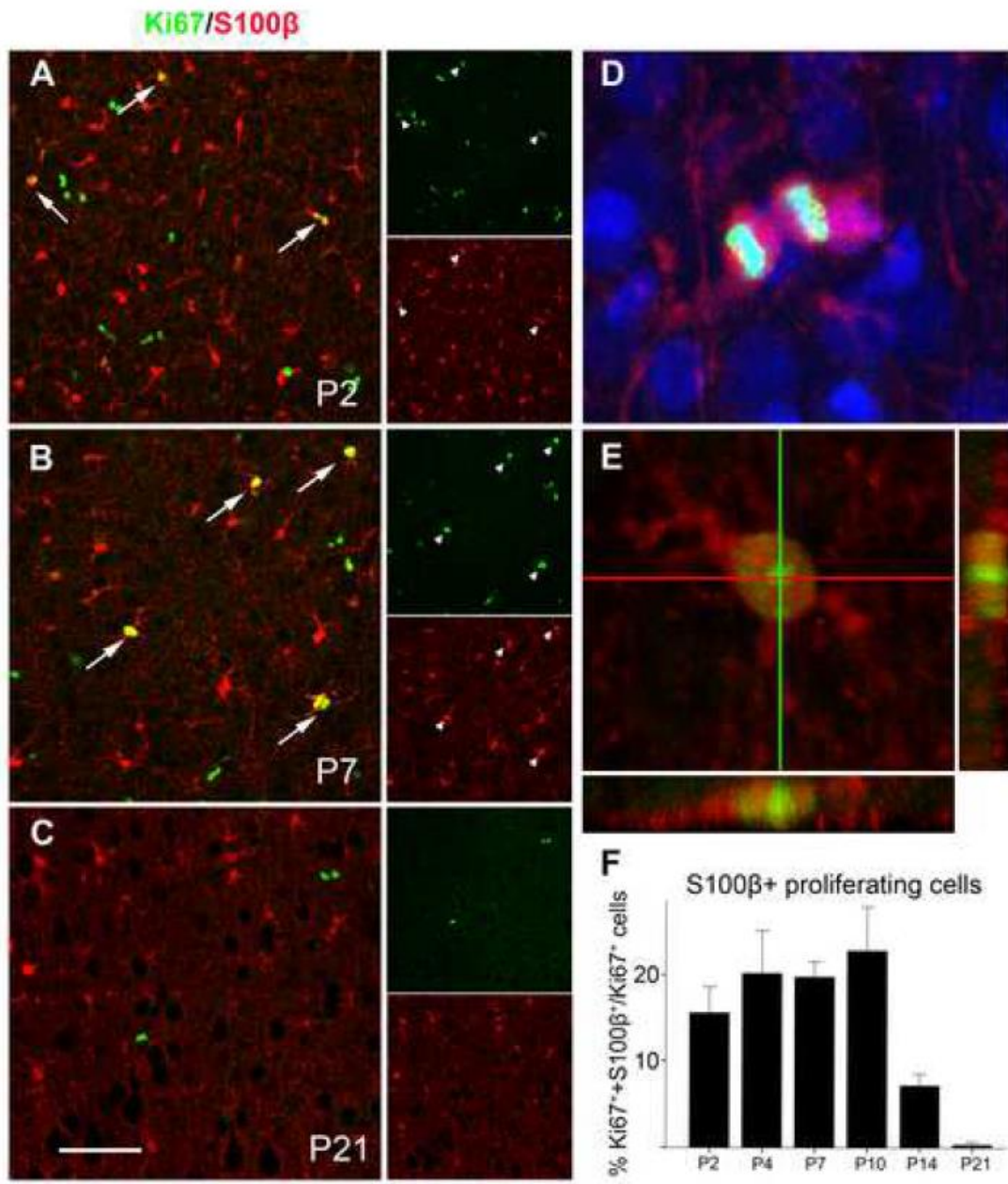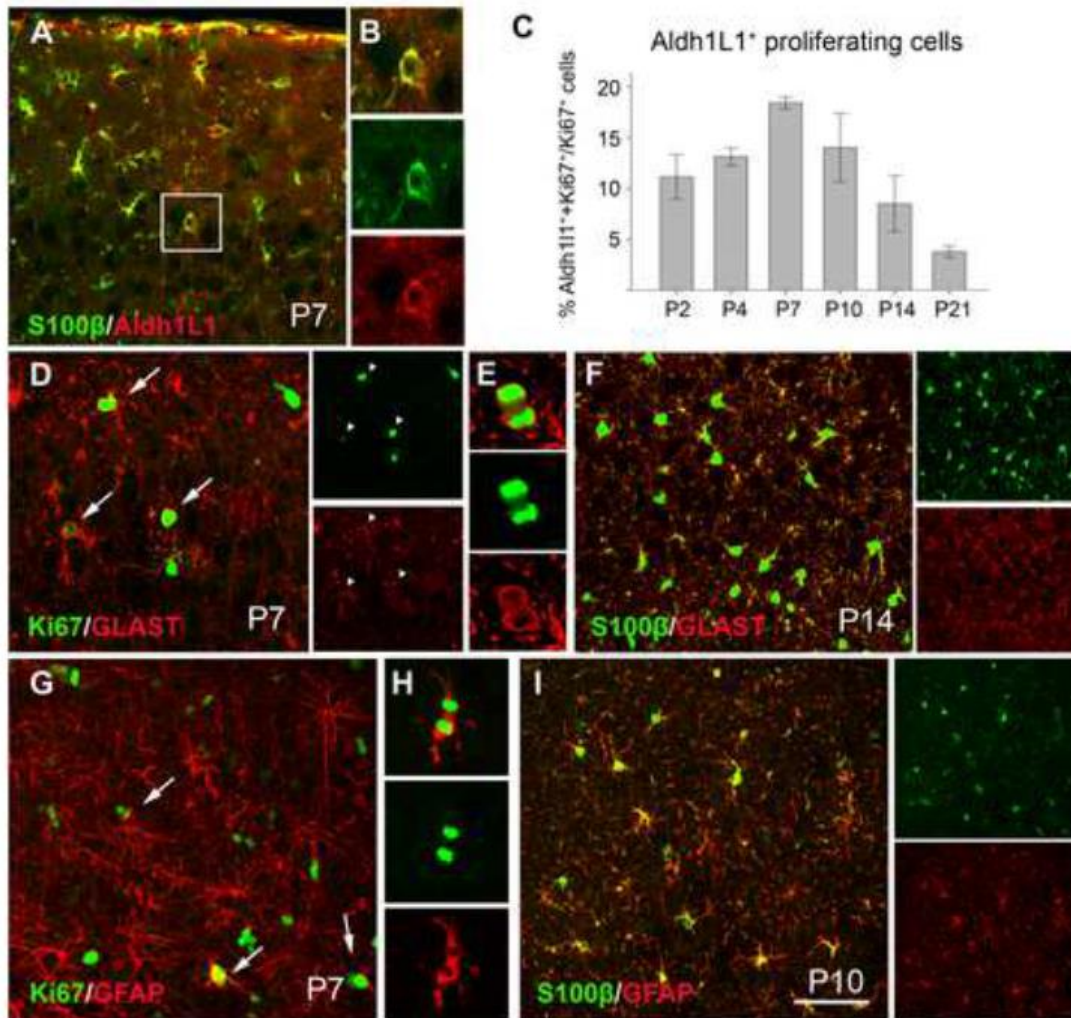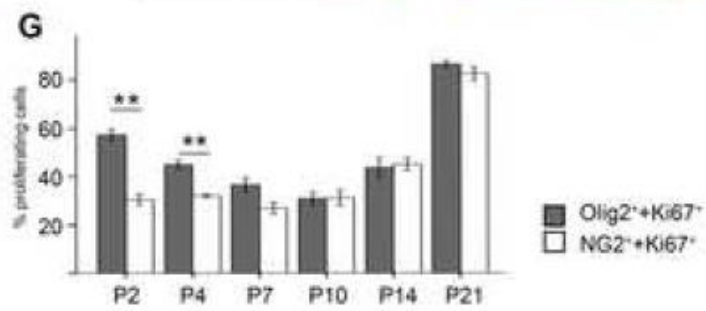
Figure 1

Figure 2

Figure 3

C

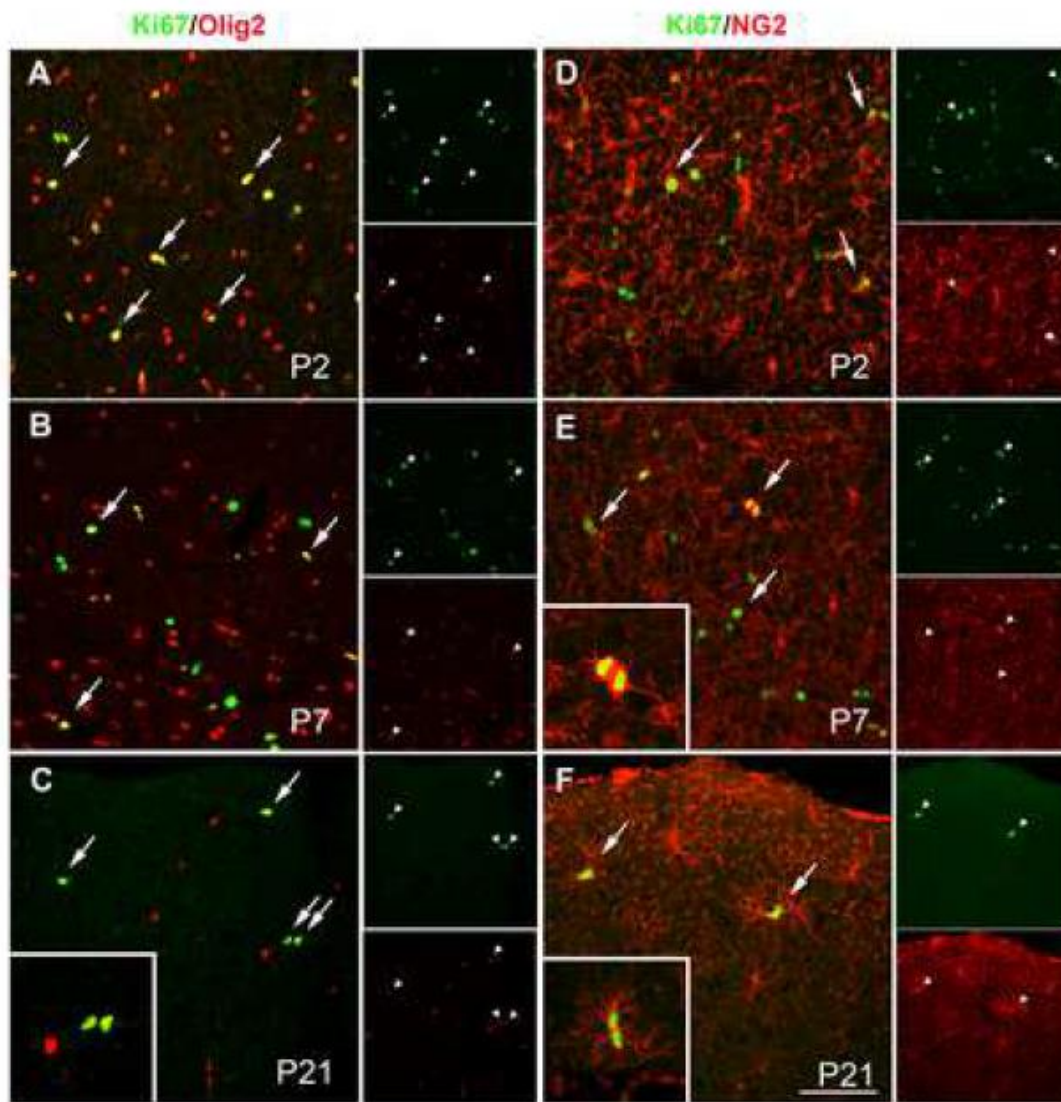Aldh1L1⁺ proliferating cells

Figure 4
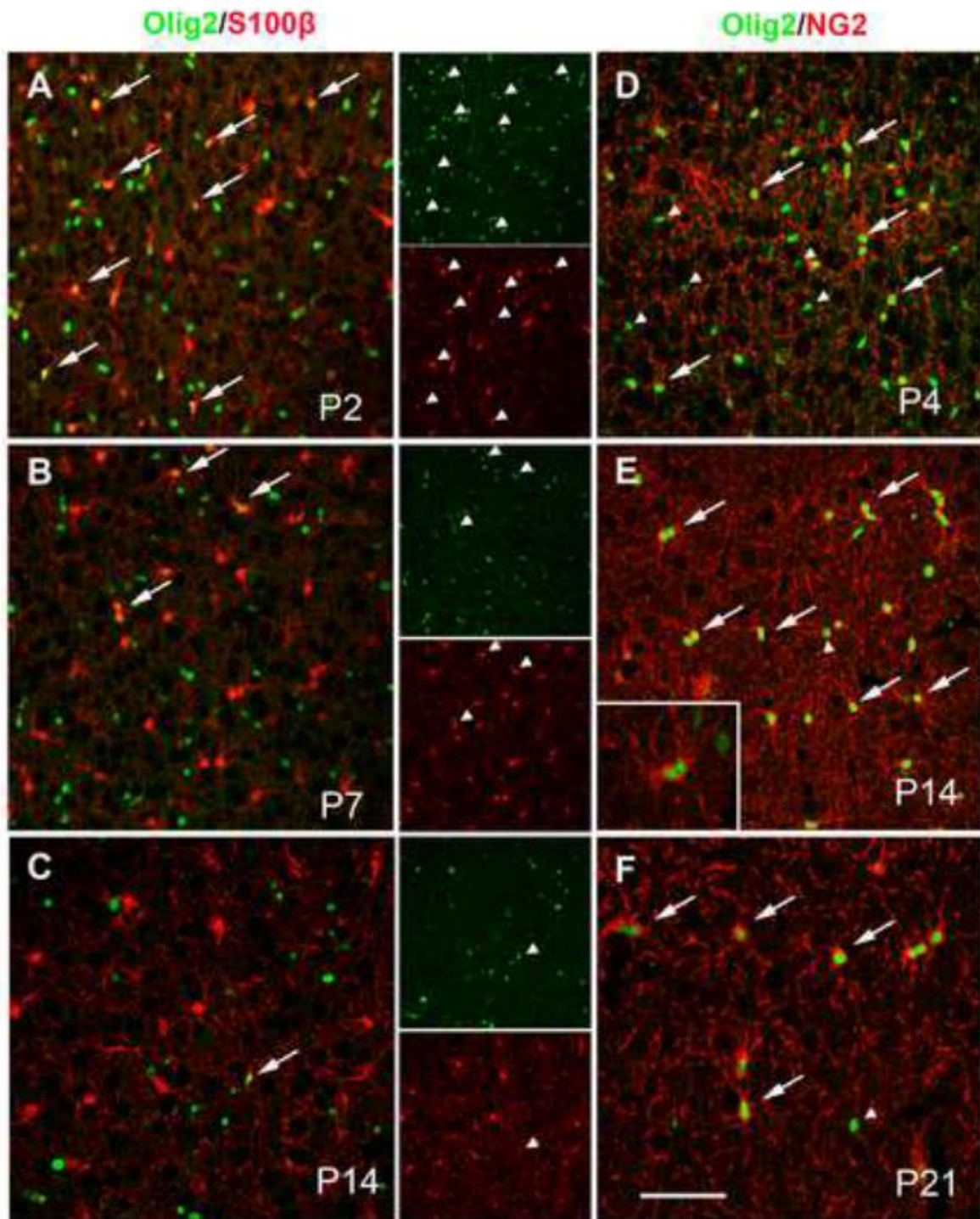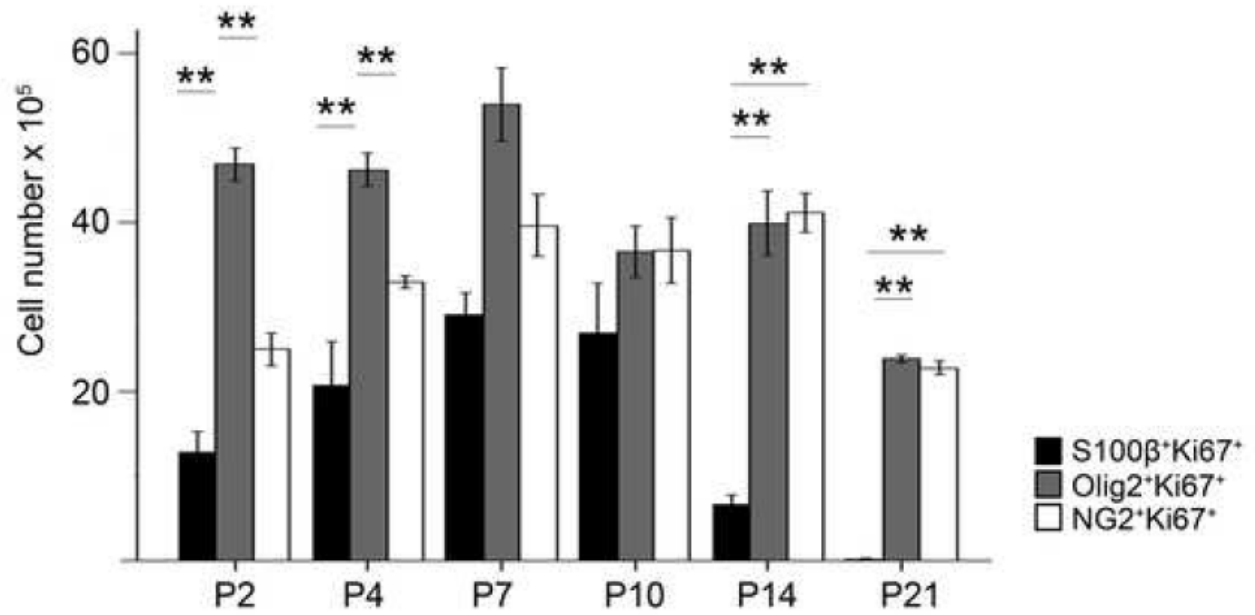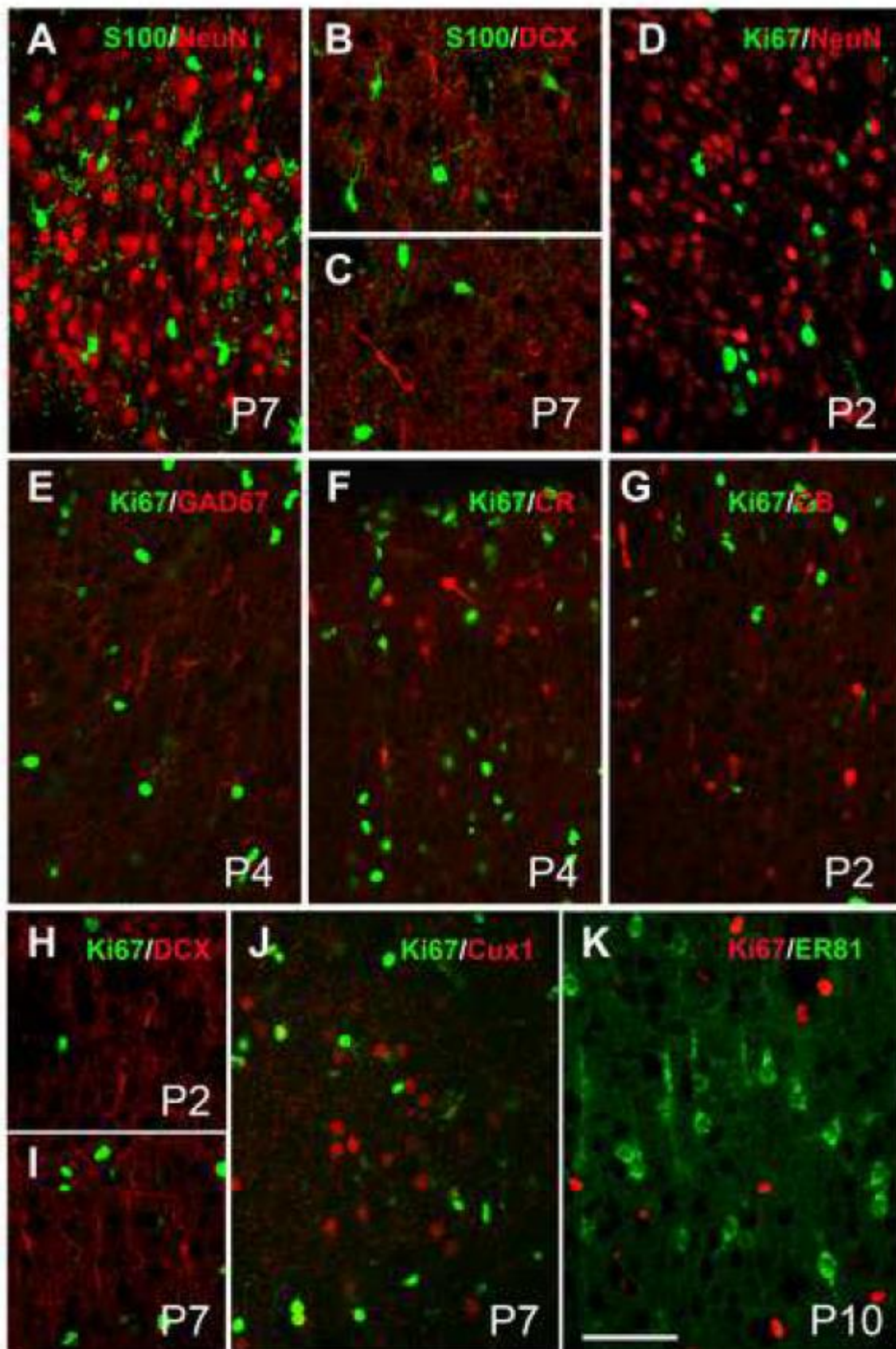
Figure 5

Olig2/S100β   Olig2/NG2

Figure 6

Estimated number of double labelled cells

Supplementary figure 1 (S1)

Supplementary figure 2 (S2)
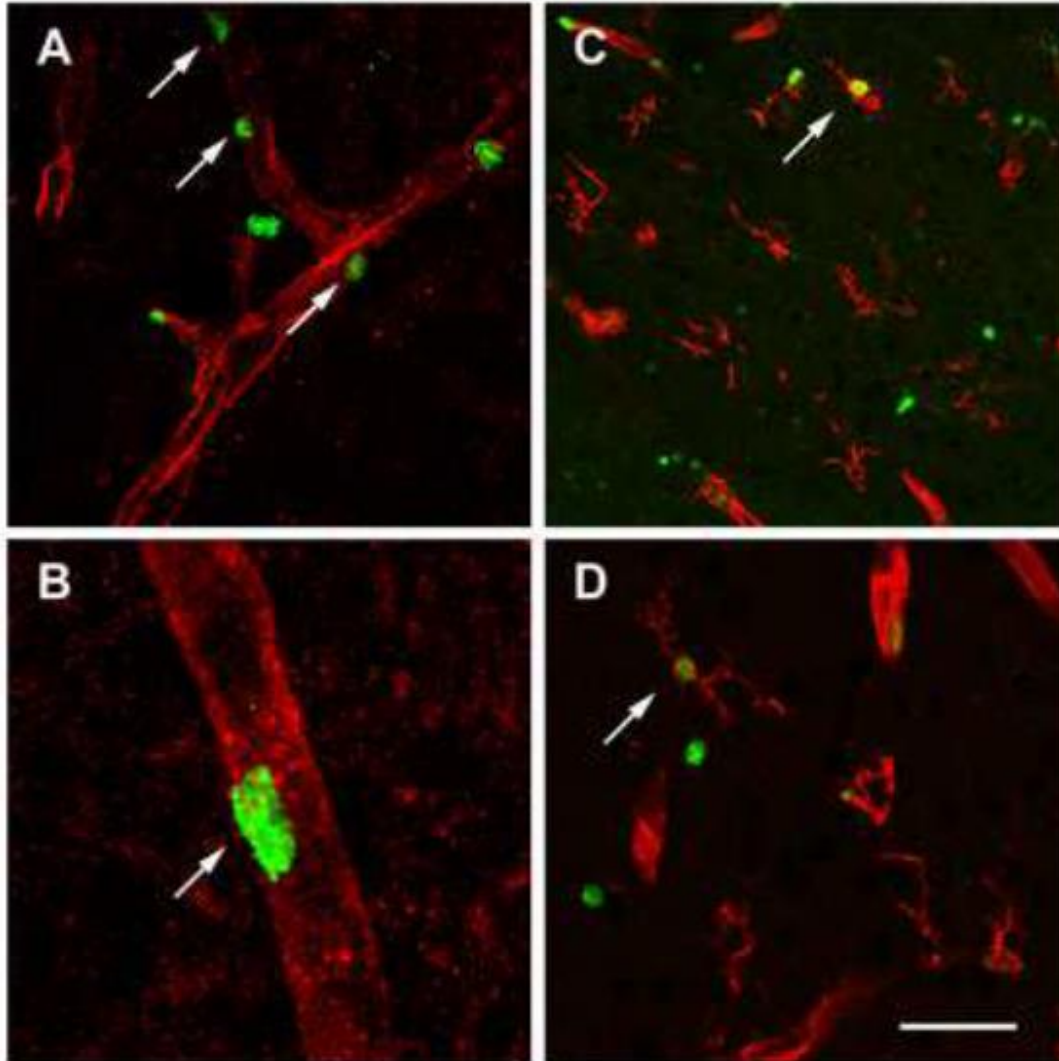
Ki67/CD31

Ki67/tomato lectin

Table 1 Synoptic information about the primary antibodies/markers used in this study

	Dilution	Source	Marker of	Reference
mouse-Aldh1L1	1:2000	Millipore	Astrocytes	Cahoy et al. 2008; Molofsky et al. 2013
mouse-CB	1:5000	Swant	GABAergic neuronal subpopulation	Celio et al. 1990; Sánchez et al. 1992
goat-CD31	1:5000	R&D Systems	Endothelial cells	Newman et al. 1990
mouse-CR	1:5000	Swant	GABAergic neuronal subpopulation	Jacobowitz and Winsky 1991
rabbit-Cux1	1:500	Santa Cruz	Upper-layer glutamatergic neurons	Nieto et al. 2004
goat-doublecortin	1:600	Santa Cruz	Migrating neurons	Francis et al. 1999; Gleeson et al. 1999
goat-GAD67	1:200	R&D Systems	GABAergic neurons	Lin et al. 1986; Spreafico et al. 1988
mouse-GFAP	1:10000	Millipore	Astrocytes	Sofroniew and Vinters 2010
goat-GLAST	1:200	Santa Cruz	Astrocytes	Lehre et al. 1995; Williams et al. 2005
rabbit-Ki67	1:1000	Thermo Scientific	Proliferating cells	Scholzen and Gerdes 2000; Taupin 2007
mouse-NeuN	1:3000	Chemicon	Neurons	Gusel'nikova and Korzhevskiy 2015
guinea pig-NG2	1:100	Gift from dr W. Stallcup	OPCs	Clarke et al. 2012; Karram et al. 2008
mouse-Olig2	1:500	Millipore	OPCs, oligodendrocytes, astrocytes (transient expression)	Kessaris et al. 2014; Ono et al. 2008
mouse/rabbit-S100β	1:1000	Sigma-Aldrich/Dako	Astrocytes	Sen and Belli 2007; Patro and Wolff 2015
Tomato Lectin	1:100	Vector	Microglial cells	Dalmau et al. 2003
Er81 riboprobe		gift from dr A. Watakabe	Layer V pyramidal neurons	Watakabe et al. 2007; Moroni et al. 2009

Table 2 Number of proliferating cells and percentage of Ki67^{+} cells expressing distinct glial markers

Age	Estimated number of Ki67^{+} cells	Density of Ki67^{+} cells (cells/mm^3)	% Ki67^{+}+S100[+]/ Ki67^{+}	% Ki67^{+}+ALDH1l1[+]/ Ki67^{+}	% Ki67^{+}+Olig2^{+}/ Ki67^{+}	% Ki67^{+}+NG2^{+}/ Ki67^{+}
P2	816389 ± 79378	30079 ± 951	15.55 ± 6.16	11.15 ± 2.21	57.32 ± 4.63	30.55 ± 4.73
P4	1027450 ± 28024	28193 ± 2582	20.16 ± 9.91	13.13 ± 0.89	45.00 ± 3.81	32.01 ± 1.42
P7	1470164 ± 256147	25424 ± 4825	19.74 ± 3.55	18.43 ± 0.59	36.63 ± 5.86	26.91 ± 4.96
P10	1179014 ± 112792	11381 ± 517	22.77 ± 10.08	14.03 ± 3.38	20.95 ± 5.14	31.12 ± 6.59
P14	912473 ± 81309	5951 ± 558	7.16 ± 2.72	8.48 ± 2.76	43.66 ± 8.39	45.10 ± 5.04
P21	275740 ± 22050	1848 ± 136	0.35 ± 0.71	3.77 ± 0.57	86.40 ± 2.77	82.53 ± 5.50